

## Effect of Solubility of Alloying Elements on Selected Properties and on the Structure of AlSi5Cu2Mg

Martina Sýkorová (0000-0001-6418-8450), Dana Bolibruchová (0000-0002-7374-9763), Marek Brůna (0000-0003-3742-7422), Mária Chalupová (0000-0003-0175-9484)

Faculty of Mechanical Engineering, University of Zilina, Univerzitná 8215/1, 010 26 Zilina, Slovakia, E-mail: [martina.sykorova@fstroj.uniza.sk](mailto:martina.sykorova@fstroj.uniza.sk), [danka.bolibruchova@fstroj.uniza.sk](mailto:danka.bolibruchova@fstroj.uniza.sk), [marek.bruna@fstroj.uniza.sk](mailto:marek.bruna@fstroj.uniza.sk), [maria.chalupova@fstroj.uniza.sk](mailto:maria.chalupova@fstroj.uniza.sk)

The paper deals with the solubility and influence of the melting method of alloying elements (Zr, Mo and Sr) on selected properties and structure of the hypoeutectic aluminum alloy AlSi5Cu2Mg. Alloying elements in the form of master alloys (AlZr20, AlMo10, and AlSr10) were melted in two different methods. The first method consisted in melting the master alloy together with the batch material in an electric resistance furnace, the second method consisted in separately melting the master alloy in an induction electric furnace and then introducing the master alloy into the molten batch. The presence of alloying elements led to an increase in the porosity in all experimental alloys, which negatively affected the resulting physical and mechanical properties.

**Keywords:** Solubility, AlSi5Cu2Mg, Zirconium, Strontium, Molybdenum

### 1 Introduction

The AlSi5Cu2Mg alloy is a relatively new alloy with significant application in the production of high-stress castings intended for the automotive industry. The AlSi5Cu2Mg alloy, having an advantageous combination of mechanical and physical properties, was designed by the manufacturer with a specific chemical composition. The AlSi5Cu2Mg alloy is characterized by a low content of Si (5 to 6.5 wt. % Si) and Ti (max. 0.03 wt. %). Due to the limited content of Ti, there is no effective modification effect through standard Al-Ti-B based modifiers, which is achieved by adding 0.04 to 0.1 wt. % Ti. In general, the physical and mechanical properties of alloys based on Al-Si-Cu-Mg are limited by the thermal stability of phases rich in Cu and Mg. Based on this fact, the operating temperature of AlSi5Cu2Mg alloys is limited to a temperature of 200 °C. One of the possibilities of effectively increasing the mechanical and physical properties of the AlSi5Cu2Mg alloy is the use of alloying elements [1-6].

Sr with a melting temperature of 777 °C is one of the most progressive modifiers of eutectic silicon in hypoeutectic and eutectic Al-Si-based alloys. It is presented in the form of master alloys with Al, usually with a content of 3.5 to 10 % Sr. In general, as the temperature of the melt increases, the rate of dissolution of the Sr-based master alloy increases, and at the same time, the modification effect of Sr starts faster. To achieve the optimal modification effect of hypoeutectic alloys based on Al-Si, it is necessary to dose 150 to 200 ppm of Sr. Premodification of Al-Si Sr alloys

results in a decrease in mechanical properties due to the formation of coarser particles of the Al4SrSi2 phase. Modification of Al-Si alloys by means of Sr can increase the porosity in the castings [2,7-12].

Zr is a transition metal with a melting point of 1855 °C. Zr finds application as an alloying element for Al-Si-Cu-Mg metals, which increases the thermal stability of specific castings for the automotive industry [13]. Zr also has modifying effect on Al-Si-Cu-Mg metals. In aluminum alloys, Zr crystallizes preferentially in the form of intermetallic phases of the type Al3Zr or AlSiZr [2]. Al3Zr phases have significantly high thermal stability and resistance to dissolution. The thermal stability of Zr-rich intermetallic phases and the grain refinement effect of Zr contribute to their being suitable for use in the development of new high-strength aluminum alloys that operate at elevated temperatures (above 200 °C) [12, 14-16]. The literature describes the metastable solubility limit as 0.87 wt. % Zr at 660 °C [17]. The solubility of Zr in Al alloys can be significantly affected by the presence of alloying elements Li, Cu, Mg, Zn, which suppress the crystallization of Al3Zr intermetallic phases due to crystallization. As a result, there is a decrease in the solubility of Zr and a decrease in the modification efficiency of Al-Si-Cu-Mg Zr alloys [17,18].

Mo is a „difficult-to-melt” metal with a high melting point of 2623 °C. Mo favorably affects the heat resistance of aluminum alloys and acts as a corrector of ferric phases, which negatively affect on the mechanical and physical properties of the aluminum alloy [19]. The maximum solubility of Mo in Al-Si alloys is 0.25 wt. % in the peritectic reaction. Adding Mo in the

form of a master alloy to Al-Si alloys leads to the formation of thermally stable Mo-based dispersoids, as a result of which there is an improvement in creep resistance at elevated temperature (above 300 °C) [2,3]. The limited solubility of Mo in aluminum leads to the formation of intermetallic phases rich in Al and Si. The presence of Mo in Al-Si-Cu-Mg alloys positively affects mechanical properties, wear resistance and corrosion resistance [20,21].

The aim of the research was to analyze the solubility and the influence of the melting method for the selected alloying elements strontium, molybdenum and zirconium on the physical properties, mechanical properties, porosity and microstructure of the hypoeutectic aluminum alloy AlSi5Cu2Mg [2]. Alloying elements were added to the melt in the form of master alloys AlSr10, AlZr20 and AlMo10. Master alloys based on AlZr20 and AlMo10 belong to difficult-to-melt master alloys. Their melting in an electric resistance furnace, together with the batch, leads to an increase in temperature and holding time at a given temperature in order to ensure their complete dissolution. These metallurgical changes in the melt preparation process lead to a deterioration of the resulting mechanical and physical properties due to a negative

increase of porosity. One of the ways to effectively melt Zr and Mo-based master alloys is the use of induction heating. Induction melting causes alternating currents to be induced in the batch, as a result of which the batch heats up and melts relatively quickly. During melting, the metal is also electro-dynamically mixed by the action of eddy currents, which achieves a uniform chemical composition of the bath. Melting master alloys separately from the batch could lead to a positive improvement of the mechanical and physical properties of the AlSi5Cu2Mg alloy. The master alloys were melted in two different methods, in an electric resistance/induction furnace in order to characterize the effect of changing the metallurgical method of melt preparation on the properties of the AlSi5Cu2Mg alloy.

## 2 Materials and Methods

For the experimental work was chosen the non-normalized hypoeutectic aluminum alloy AlSi5Cu2Mg. The chemical composition of the experimental AlSi5Cu2Mg alloy is shown in Tab.1. The specific chemical composition of experimental alloy is specified by the supplier company.

**Tab. 1** Chemical composition of reference alloy AlSi5Cu2Mg [wt. %]

Si	Cu	Mg	Mn	Sr	Mo	Zr	Ti	Mn/Fe	Al
5.40	1.85	0.29	0.03	0.008	0.0006	0.0006	0.013	0.09	Bal.

The AlSi5Cu2Mg alloy was melted in an electric resistance furnace. Experimental alloys were prepared by alloying 0.12 wt. % Sr, 0.20 wt. % Zr and 0.15 wt. % Mo. The stated contents of alloying elements were selected based on the literature survey and our previous investigations [3,7,12,20]. Additive elements in the form of master alloys AlZr20, AlMo10, and AlSr10 were melted in two different methods and introduced into the melt at a temperature of 770 °C ± 5 °C [3]. The first method consisted in melting the master alloy together with the batch in an electric resistance furnace at the melting temperature. In this case, the experimental alloys were labeled Sr/Zr/Mo-R. The second method consisted of melting the master alloy in an electric induction furnace and then introducing the molten master alloy into the batch. In the second case, the experimental alloys were labeled Sr/Zr/Mo-I. The chemical composition of the experimental alloys is

**Tab. 2** Chemical composition of experimental alloys [wt. %]

	Si	Cu	Mg	Mn	Sr	Mo	Zr	Ti	Mn/Fe	Al
<b>Sr-I</b>	5.75	1.88	0.29	0.015	0.14	0.0007	0.0007	0.012	0.12	Bal.
<b>Sr-R</b>	5.75	1.88	0.29	0.015	0.14	0.0007	0.0007	0.013	0.15	Bal.
<b>Zr-I</b>	5.60	1.88	0.29	0.015	0.009	0.0006	0.19	0.013	0.14	Bal.
<b>Zr-R</b>	5.51	1.87	0.30	0.015	0.008	0.007	0.20	0.012	0.12	Bal.
<b>Mo-I</b>	5.72	1.92	0.29	0.015	0.007	0.13	0.0007	0.013	0.11	Bal.
<b>Mo-R</b>	5.69	1.94	0.28	0.015	0.008	0.13	0.0007	0.013	0.13	Bal.

shown in Tab. 2. The chemical composition was measured by using optical emission spectroscopy Spectrolab S. The chemical composition of the experimental alloys was evaluated on experimental samples with a diameter of 38 mm and a height of 10 mm. For each experimental variant, 3 samples were cast for chemical analysis. The experimental samples were cast in 3 stages of the casting process. The first sample was cast at the beginning of the casting process, the second sample was cast after the 3 castings were cast into the non-normalized metal mold (Fig. 1), and the third sample was cast at the end of the casting process. Three independent chemical composition measurements were made on each experimental sample. For each experimental alloy, the resulting chemical composition was determined by the arithmetic average of the 9 measurements.

The experimental samples were cast using gravity casting technology into a not standardized metal mold (Fig. 1). The material of the metal mold was steel [2]. Metal mold was coated with a graphite powder [2]. The casting temperature was  $740\text{ }^{\circ}\text{C} \pm 5\text{ }^{\circ}\text{C}$  and the mold temperature was  $180\text{ }^{\circ}\text{C} \pm 5\text{ }^{\circ}\text{C}$ . The temperature of the metal mold was maintained by flame [2]. The experimental alloy was not metallurgically affected or degassed in the preparation process [3].

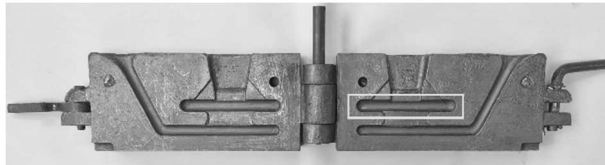


**Fig. 1** Metal mold with the marked extraction place for the tensile test bar (yellow field)

The experimental samples were subjected to an evaluation of the area fraction of porosity. The area fraction of porosity was evaluated with the graphic software Quick Photo Industrial 3.2. The size of measurement area was  $2460\text{ }\mu\text{m} \times 1700\text{ }\mu\text{m}$ . The measurement area was consistent for all samples. Samples for the evaluation of the area fraction of porosity were taken from the same location as tensile test bar, the extractions place for the tensile test bar is marked with a yellow field in Fig. 1. For each experimental sample, five randomly selected locations were evaluated.

The conductivity of the experimental alloys was evaluated by the alloy manufacturer's method. This method was based on the measurement of the electrical conductivity using a Sigma Check 2 conductometer with a touch sensor. Five measurements were performed for each experimental alloy. The values of the electrical conductivity ( $\sigma$ ) were substituted into the empirical equation (1) to calculate the thermal conductivity ( $\lambda$ ) of the experimental samples [2]:

$$\lambda = 4.29 \cdot \sigma - 13.321 [\text{W} \cdot \text{m}^{-1} \cdot \text{K}^{-1}] \quad (1)$$

The mechanical properties of the experimental alloys were determined by a static tensile test. In accordance with the EN ISO 6892-1 standard, a universal tearing device Inspekt desk 50 kN was used to perform the tensile test. A series of five test circular rods with a shank diameter of 8 mm were made for each experimental variation [2]. Fig. 2 shows the scheme of the tensile test bar. The tensile test bars were obtained from the casting extraction place (Fig. 2) by cutting and subsequent turning.

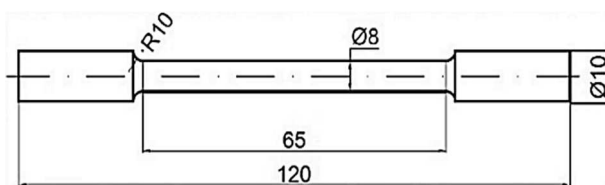


**Fig. 2** The scheme of the tensile test bar

The Brinell hardness test was used to determine the experimental alloy's hardness in accordance with EN ISO 6506-1. The measurements were carried out with a Brinell Innovatest Nexus 3000 hardness tester according to HBW 5/250/10 (indentation body - 5 mm diameter carbide ball/ load size 250 kp/ load time 10 s) [2]. Five measurements were made for each variant of the experiment [2].

The microstructure of the experimental alloys was evaluated with a Neophot 32 optical light microscope and a TESCAN LMU II scanning electron microscope with a BRUKER EDX analyzer [2]. Experimental samples were prepared by standard methods. Samples with the most appropriate combination of mechanical and physical properties were subjected to microstructural analysis.

### 3 Evaluation of Area Fraction of Porosity

The effect of Sr, Zr and Mo elements on the porosity of the experimental AlSi5Cu2Mg alloy was defined by the area fraction of porosity. The area fraction of porosity of the experimental alloys depending on the additive element and the method of melting and introduction of the additive elements into the melt are processed into a graphical dependence Fig. 3. [2]

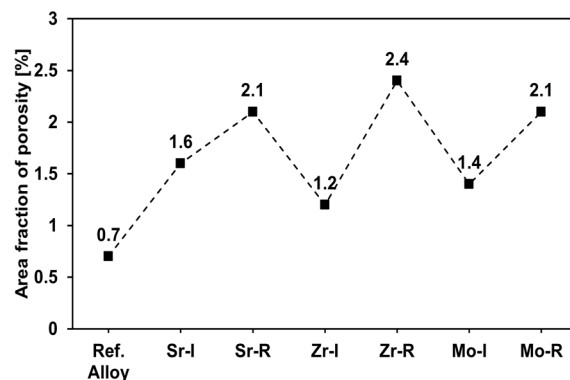


**Fig. 3** Area fraction of porosity of experimental alloys

On each experimental alloy, five different locations were selected for the measurement. The area fraction of porosity of the experimental alloys represents the average of five measurements. Pores were identified in the plane of the metallographic cut through the "phase change" function, as shown by the red areas in Fig. 4. [2]

The area fraction of the porosity of the experimental alloys with the Sr, Zr, and Mo Addition increased substantially compared to the reference alloy AlSi5Cu2Mg [2,3]. The largest increase in surface porosity by 243 % compared to the reference alloy was recorded by the Zr-R alloy. Conversely, the smallest increase in surface porosity of 71 % was recorded by the Zr-I alloy compared to the reference alloy. The area fraction of the porosity of the experimental alloys differs significantly also due to the method of melting

and introduction of alloying elements into the melt. The area fraction of porosity of the Sr-I, Zr-I, and Mo-I alloys decreased compared to the surface porosity of Sr-R by 24 %, Zr-R by 50 % and Mo-R by almost 34 %. The increased porosity of Sr-R, Zr-R, and Mo-R

alloys could be significantly influenced by the metallurgical process of melt preparation [2]. The melting temperature and the holding time at the given temperature were slightly increased due to the complete melting of the master alloy AlSr10, AlZr20, and AlMo10 [2,23,24].

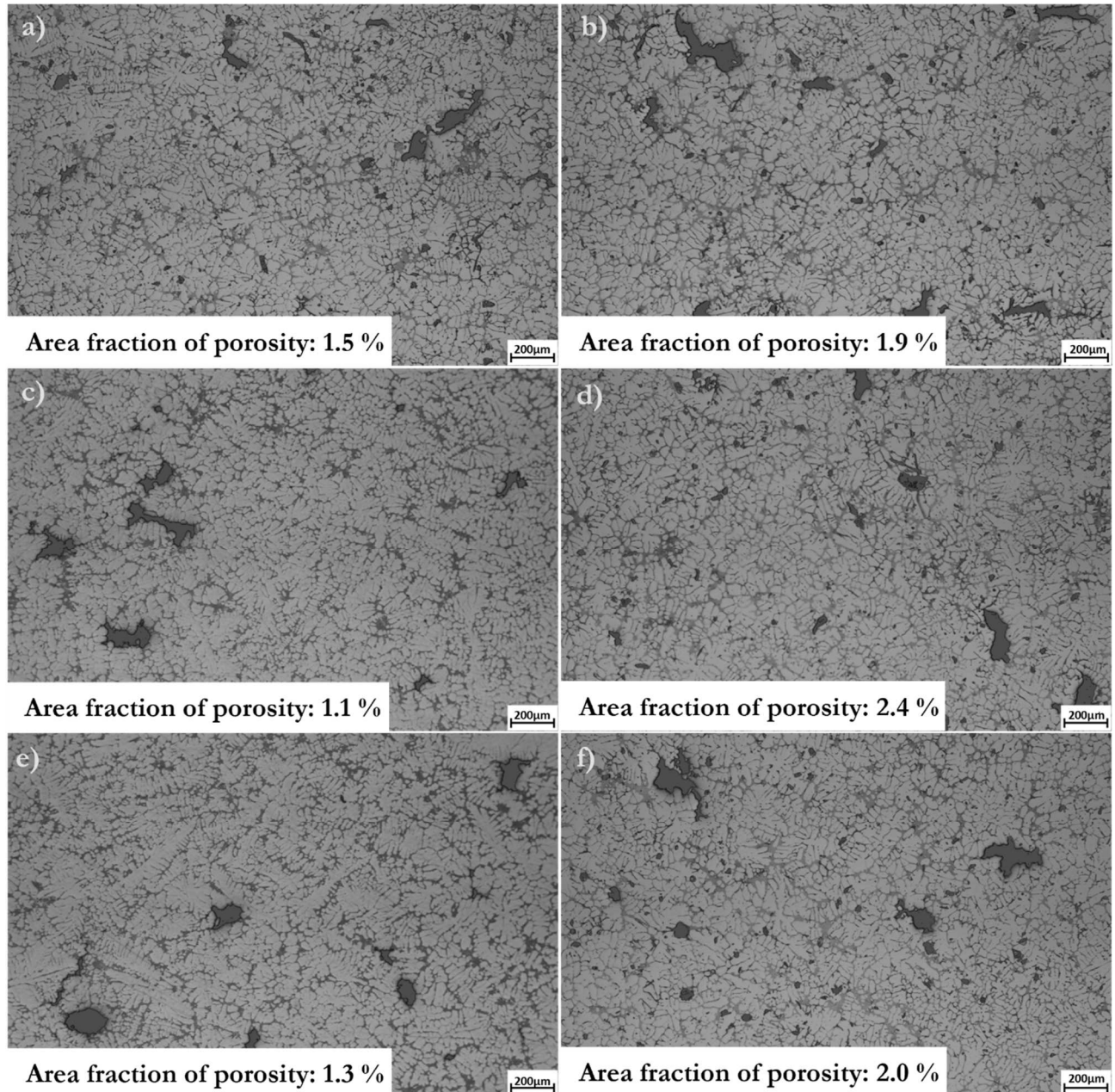


**Fig. 4** Evaluation of area fraction of porosity of experimental alloys: a) Sr-I, b) Sr-R, c) Zr-I, d) Zr-R, e) Mo-I, f) Mo-R (0.5 % HF etch.)

#### 4 Evaluation of Physical Properties

The electrical and thermal conductivity of the experimental alloys was processed into a graphical dependence Fig. 5. Due to the influence of the alloying elements Sr, Zr and Mo, there is a decrease in the physical properties of the studied alloy. The largest decrease in physical properties by an average of 18 % was recorded in the Zr-R alloy compared to the

reference alloy. The smallest decrease of approximately 7 % compared to the reference alloy was observed in the Sr-R alloy. The electrical and thermal conductivity of experimental alloys with the addition of Sr and Mo does not fundamentally change depending on the method of melting and introduction of the additive element into the melt. On the contrary, the physical properties of the experimental Zr-R alloy decreased by an average of 10 % compared to Zr-I.

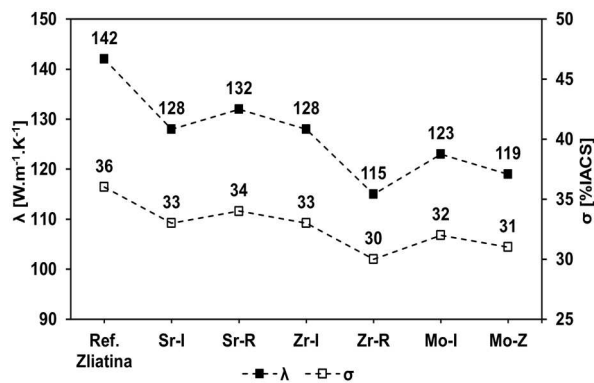


Fig. 5 Physical properties of experimental alloys

In general, any alloying element added to an aluminum alloy negatively affects the physical properties [2]. Alloying elements block the movement of electrons, resulting in a decrease in the physical and electrical properties of the aluminum alloy. The physical properties were also significantly influenced by the porosity present [2]. The porosity of the casting depends both on the amount of hydrogen present in the melt and on the metallurgical process of the melt preparation [2, 3]. In order to completely melt the AlSr10, AlZr20, and AlMo10 master alloys, it was necessary to increase the melting temperature and extend the holding time at the given temperature. The changes made to the metallurgical process led to an increase in the porosity of the experimental alloys. The pores acted as "impurities" and prevented the free passage of electrons through the environment, causing a decrease in physical properties [25].

## 5 Evaluation of Mechanical Properties

The resulting values of the mechanical properties are shown in Fig. 6 and represent the average of 5 measurements [2,3]. Alloys with the addition of Sr do not show significant changes in mechanical properties compared to the reference alloy [2]. The Sr-I alloy shows a negligible decrease in  $R_m$  and HBW compared to the Sr-R alloy. The  $R_{p0.2}$  value, on the other hand, slightly increased compared to the Sr-R alloy. The ductility of the experimental alloys with Sr addition was identical. The addition of Zr to the reference AlSi5Cu2Mg alloy had a more significant effect on the resulting mechanical properties. The mechanical properties of Zr-I increased slightly compared to the reference alloy, Sr-R and Sr-I. The highest  $R_{p0.2}$  and HBW values were achieved with the Zr-I alloy. Compared to the reference alloy  $R_{p0.2}$ , HBW increased by approximately 9 %. On the contrary, the mechanical properties of Zr-R decreased compared to the reference alloy AlSi5Cu2Mg, Sr-R, Sr-I, and at the same time there was a significant decrease compared to the Zr-I alloy.

The Zr-R alloy had the lowest values of  $R_m$  and  $R_{p0.2}$ , which decreased by approximately 12 % compared to the Zr-I alloy. The decrease in the mechanical properties of the Zr-R alloy could be caused by the presence of hard and brittle Zr-rich intermetallic phases [2]. Alloys with the addition of Mo achieved the best mechanical properties. HBW did not change significantly due to the method of melting and introduction of the AlMo10 master alloy into the batch material. The values of the mechanical properties  $R_m$  and  $A_5$  of the experimental Mo-I alloy slightly increased compared to the Mo-R alloy. The largest increase in  $R_m$  and  $A_5$  (10 % and 63 %) compared to the reference alloy was achieved for the Mo-I alloy.

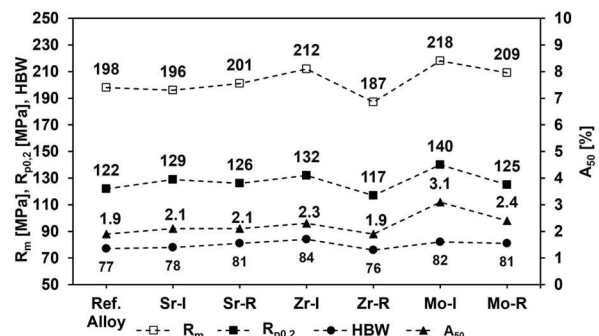


Fig. 6 Mechanical properties of experimental alloys

Based on the obtained results, it can be concluded that induction melting of AlMo10 and AlZr20 master alloys was more effective in terms of the achieved mechanical properties for alloys with the addition of Mo and Zr. Master alloys AlMo10 and AlZr20 are characterized by a high melting temperature. When introducing the master alloys into the melt in the electric resistance furnace, it was necessary to increase the melting temperature and the holding time at the given temperature in order to ensure complete melting of the AlZr20 and AlMo10 master alloys. Due to the change in the metallurgical process of melt preparation, the porosity increased which led to a negative effect on the mechanical and physical properties of experimental alloys [2]. Induction melting of AlZr20 and AlMo10 master alloys resulted in the formation of eddy currents, which caused relatively rapid heating and melting of the master alloys. As a result of the melting of the master alloys separately, it was not necessary to change the parameters of the metallurgical process of the melt preparation, which would lead to an increase in the porosity [2,3].

## 6 Evaluation of Microstructure and EDX Analysis

The microstructure of the AlSi5Cu2Mg alloy in the as-cast state consists of primary  $\alpha$ -phase, eutectic Si,

and Cu and Fe-rich intermetallic phases (Fig. 7) [2]. Due to the fact that the reference alloy was supplied in a pre-modified state, eutectic Si was observed in the form of imperfectly round grains. Fe-based intermetallic phases were precipitated in the form of gray plates with split ends [2].

The microstructures of the experimental Sr-I and Sr-R alloys in the cast state can be seen in Fig. 8. Cu-based intermetallic phases were observed in the metallographic cut plane in the form of a ternary eutectic with a compact morphology. Eutectic Si is excluded in the form of almost perfectly round grains due to the modifying effect of Sr [2]. Fe-based intermetallic phases were present in both experimental alloys.

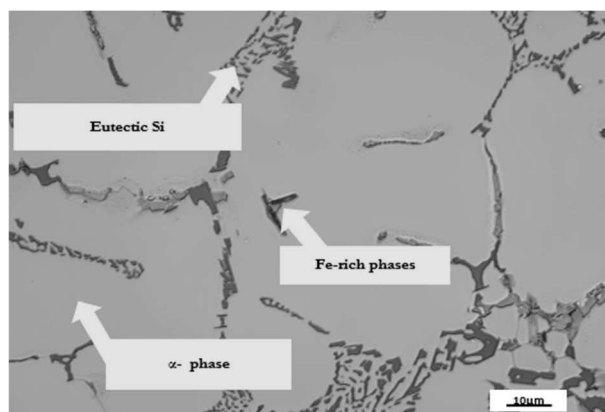


**Fig. 7** Microstructural evaluation of AlSi5Cu2Mg alloy ( $H_2SO_4$  etch.)

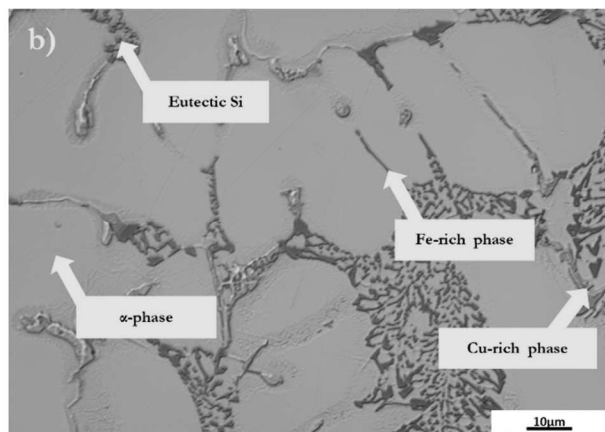
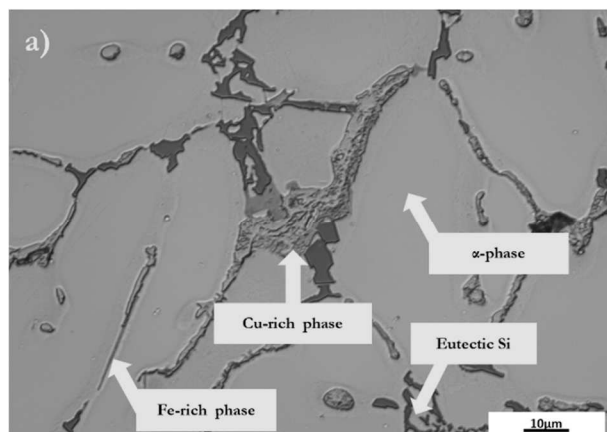
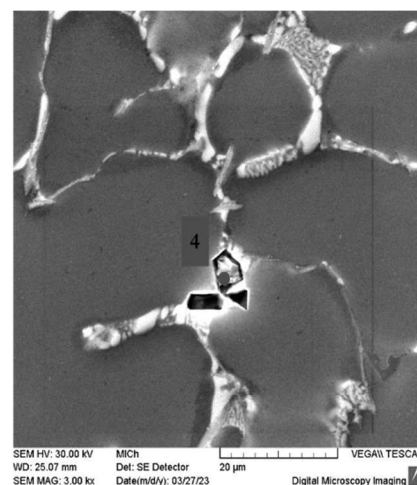


**Fig. 8** Microstructural evaluation of experimental alloys: a) Sr-I, b) Sr-R ( $H_2SO_4$  etch.)

In the experimental Sr-I alloy, the presence of sharp-edged formations was detected in the matrix (Fig. 9). By EDX analysis, these structural components were identified as particles with a high concentration of Sr. Considering this fact, it can be concluded that in the case of the experimental Sr-I alloy, the AlSr10 master alloy did not completely dissolve. An increased concentration of Cu-rich intermetallic phases was demonstrated in the vicinity of sharp-edged particles. On the contrary, based on the EDX analysis of the experimental Sr-R alloy, the presence of sharp-edged formations that could be identified as Sr particles was not demonstrated. In this case, it can be concluded that complete dissolution of Sr in the melt occurred. The presence of sharp-edged formations could lead to a decrease in the physical properties and  $R_m$  of the experimental Sr-I alloy compared to Sr-R [3].

As can be seen in Fig. 10, the microstructure of the experimental Zr-I and Zr-R alloys in the as-cast state consists of primary  $\alpha$ -phase and eutectic Si. Intermetallic phases based on Fe and Cu were present in the metallographic cut plane of the experimental alloys Zr-I and Zr-Z. Intermetallic phases rich in Cu were observed in the form of a ternary eutectic with a compact morphology.



Spectrum: 4						
El	AN	Series	unn. C [wt.%]	norm. C [wt.%]	Atom. C [at.%]	Error (1 Sigma) [wt.%]
Mg	12	K-series	6.09	6.32	8.43	0.39
Al	13	K-series	63.87	66.31	79.67	3.23
Fe	26	K-series	1.07	1.11	0.64	0.07
Cu	29	K-series	10.56	10.97	5.59	0.31
Sr	38	K-series	14.73	15.29	5.66	0.55
Total:			96.32	100.00	100.00	

**Fig. 9** EDX analysis of Sr particles of experimental alloy Sr-I



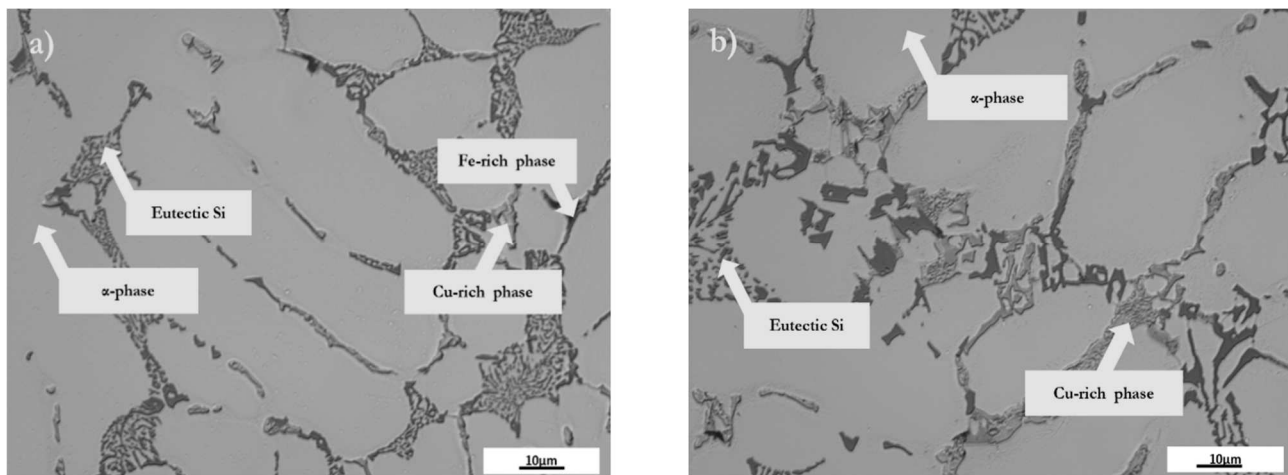
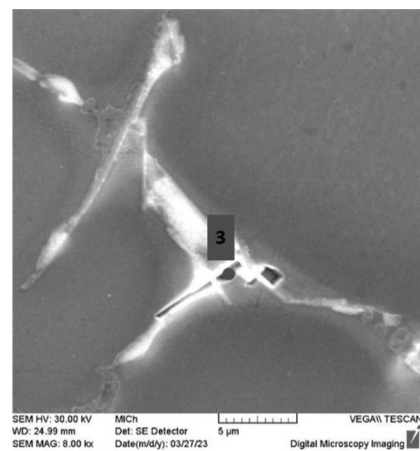


**Fig. 10** Microstructural evaluation of experimental alloys: a) Zr-I, b) Zr-R ( $H_2SO_4$  etch.)

The presence of Zr-rich intermetallic phases was identified by EDX analysis (Fig. 11). The Zr-phases present in the experimental Zr-I and Zr-R alloys were identified as  $AlSiZr$  and  $Al_3Zr$ -based phases. Intermetallic phases based on Zr were excluded in the form of individual thicker needles. The presence of hard and brittle intermetallic phases based on Zr could lead to a decrease in the physical and mechanical properties of the Zr-I and Zr-R Experimental alloys [2]. EDX analysis showed an increased concentration of Cu-rich intermetallic phases around the Zr-based intermetallic phases.

The microstructures of the experimental Mo-I and Mo-R alloys in the as-cast state are shown in Fig. 12. Intermetallic phases based on Fe and Cu can be observed. The experimental Mo-I alloy was characterized by a local thickening of eutectic Si compared to Mo-R.

EDX analysis proved the presence of intermetallic phases rich in Mo (Fig. 13). An increased concentration of Mg and Fe-rich intermetallic phases was detected in the vicinity of phases rich in Mo. The presence of Mo reduces the adverse effect of Fe in aluminum alloys and thus acts as a corrector of Fe phases.



**Spectrum: 3**

El	AN	Series	unn. C [wt.%]	norm. C [wt.%]	Atom. C [at.%]	Error (1 Sigma) [wt.%]
Mg	12	K-series	1.43	1.29	1.67	0.12
Al	13	K-series	74.86	67.84	78.89	3.78
Si	14	K-series	9.12	8.26	9.23	0.45
Fe	26	K-series	6.52	5.91	3.32	0.21
Cu	29	K-series	8.46	7.66	3.78	0.26
Zr	40	K-series	9.97	9.03	3.11	0.49
<b>Total:</b>			<b>110.35</b>	<b>100.00</b>	<b>100.00</b>	

**Fig. 11** EDX analysis of Zr intermetallic phase

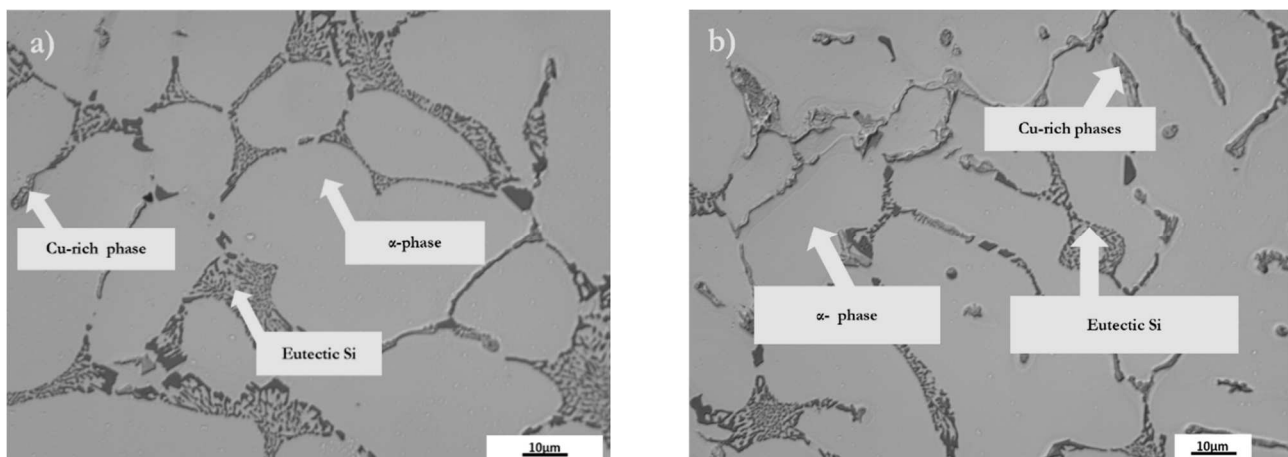


**Fig. 12** Microstructural evaluation of experimental alloys: a) Mo-I, b) Mo-R ( $H_2SO_4$  etch.)

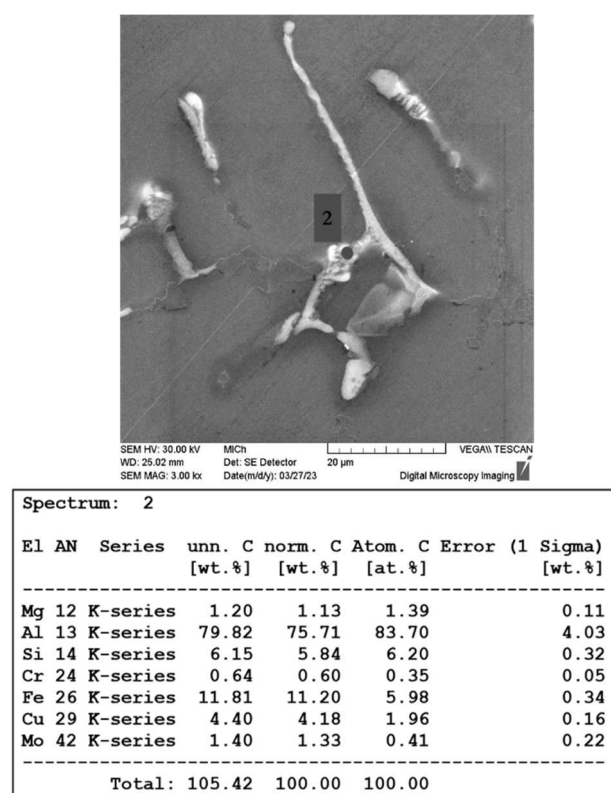


Fig. 13 EDX analysis of Mg intermetallic phases

## 7 Conclusion

The aim of the work was to analyze the solubility of selected elements (Sr, Zr, Mo) and the influence of the method of their melting on porosity, physical/mechanical properties and microstructure of reference alloy AlSi5Cu2Mg. Based on the obtained results, the following conclusions can be stated:

- The method of melting of the alloying elements had a significant effect on the porosity of the investigated alloys. Porosity of Sr-R, Zr-R and Mo-R alloys increased substantially compared to Sr-I, Zr-I and Mo-I alloy probably due to the change in the metallurgical process of melt preparation. The change in the melt preparation process consisted in increasing the temperature and holding time at a given temperature to ensure the complete dissolution of the master alloys in the batch during the melting in an electric resistance furnace. As is generally known, porosity negatively affects the resulting physical and mechanical properties of aluminum castings. The presence of pores blocks the transfer of electrons through the medium [2]. As a result, there is an unfavorable decrease in the physical properties of the casting.

- The addition of Sr, Mo and Zr negatively affected the physical properties of the reference alloy AlSi5Cu2Mg in the cast state [2]. Alloying elements generally act as a barrier for the free movement of electrons through the environment, resulting in an unfavorable decrease in physical properties. Depending on the method of melting, no significant changes in the physical properties of the experimental alloys with the addition of Sr and Mo were noted. On the contrary, the physical properties of the Zr-I alloy have increased compared to Zr-R.
- The mechanical properties of the experimental alloys with the Sr, Zr, and Mo addition increased compared to the reference alloy AlSi5Cu2Mg. Considering the achieved mechanical properties, it was demonstrated that the induction melting of AlMo10 and AlZr20 master alloys was more effective. An important role in this case is played by the rate of the porosity, which increased in the case of Zr-R and Mo-R alloys as a result of the change in the metallurgical process of melt preparation [2]. Experimental alloys with Sr addition did not show significant changes in selected properties depending on the method of melting the AlSr10 master alloys. The best mechanical properties from the studied set of alloys were achieved by the experimental Mo-I alloy. Conversely, the worst mechanical properties were achieved by the Zr-R alloy.
- An increased concentration of phases rich in Cu and Fe was detected in the experimental alloys. By EDX analysis, particles with a high concentration of Sr were identified in the matrix of the experimental Sr-I alloy, which were excluded in the form of sharp-edged formations. In this case, the AlSr10 master alloy did not completely dissolve.
- Similarly, to experimental alloys with Sr addition, an increased concentration of phases rich in Fe and Cu was recorded in experimental alloys with Zr addition in the vicinity of the Zr-rich intermetallic phases. EDX analysis proved the presence of hard and brittle intermetallic phases based on Zr, which



were excluded in the form of needles. Hard and brittle intermetallic phases based on Fe and Zr could lead to a decrease in physical and mechanical properties of Zr-R and Zr-I alloys.

- The Mo-I alloy was characterized by local thickening of eutectic Si compared to Mo-R. EDX analysis detected the presence of Mo-rich phases in the vicinity of which an increased concentration of Fe phases was recorded.
- Based on the above conclusions, it can be demonstrated that the melting of AlMo10 and AlZr20 master alloys is more efficient in terms of the obtained results in an electric induction furnace. On the other hand, with the relatively easy-to-melt AlSr10 master alloy, the method of melting does not play a significant role.

### Acknowledgement

***This research was created within the project of the grant agency VEGA 1/0160/22 and Grant System of University of Žilina No. 1/2021 (14862). The authors thank for the support.***

***This article was funded by the University of Žilina project 313011ASY4 „Strategic implementation of additive technologies to strengthen the intervention capacities of emergencies caused by the COVID -19 pandemic“.***

### References

- [1] BENEDYK, J. C. (2010). Aluminium Alloys for Lightweight Automotive Structures. *Materials, Design and Manufacturing for Lightweight Vehicles*, pp. 79-113. Woodhead Publishing, ISBN 9781845694630
- [2] BOLIBRUCHOVÁ, D., SÝKOROVÁ, M., BRŮNA, M., MATEJKA, M., ŠIRANEC, L. (2023). Effect of Zr Addition on Selected Properties and Microstructure of Aluminum Alloy AlSi5Cu2Mg. *International Journal of Metalcasting*, Vol. 17, pp. 2598-2611. DOI: 10.1007/s40962-023-01048-z
- [3] BOLIBRUCHOVÁ, D., SÝKOROVÁ, M., ŠIRANEC, L. (2023). Vplyv Sr, Zr a Mo na vybrané vlastnosti AlSi5Cu2Mg zliatiny. *Technológ*, DOI: 10.26552/tech.C.2023.2.8
- [4] SHIN, J., TAEHYEONG, K., DONGEUNG, K., DONGKWON, K., KITAE, K. (2017). Castability and Mechanical Properties of New 7xxx Aluminum Alloys for Automotive Chassis/Body Applications. *Journal of Alloys and Compounds*, Vol. 698, pp. 577-590. ISSN 0925-8388
- [5] CZERWINSKI, F. (2020). Thermal Stability of Aluminum Alloys. *Materials*, Vol. 13, No. 15, DOI: 10.3390/ma13153441
- [6] BEROUAL, S., BOUMERZOU, Z., PAILLARD, P., BORJON-PIRON, Y. (2019). Effect of Heat Treatment and Addition of Small Amounts of Cu and Mg on the Microstructure and Mechanical Properties of Al-Si-Cu and Al-Si-Mg Cast Alloys. *Journal of Alloys and Compounds*, Vol. 784, pp. 1026-1035. ISSN 0925-8388
- [7] BOLIBRUCHOVÁ, D., PASTIRČÁK, R. (2018). *Zlievarenská metalurgia neželezných kovov*, EDIS, Žilina. ISBN 978-80-554-1463-8
- [8] BARRIRERO, J., ENGSTLER, M., GHAFOR, N., JONGE, N., ODÉN, M., MUECKLICH, F. (2014). Comparison of Segregation Formed in Unmodified and Sr-modified Al-Si Alloys Studied by Atom Probe Tomography and Transmission Electron Microscopy. *Journal of Alloys and Compounds*, pp. 410-421. DOI: 10.1016/j.jallcom.2014.05.121
- [9] ZHANG, W., MA, S., WEI, Z., BAI, P. (2019). The Relationship between Residual Amount of Sr and Morphology of Eutectic Si Phase in A356 Alloys. *Materials*, Vol. 12, No. 19, DOI: 10.3390/ma12193222
- [10] OMRAN, A., ALI, M., KH, M., EZZELDIEN, M. (2018). Effect of Strontium Content on the Mechanical Properties of Hypo and Hyper Al-Si Cast Alloys. *Journal of Al-Azhar University Engineering Sector*, Vol. 13, No. 49, pp. 1322-1331. ISSN 1687-8418
- [11] LIPÍŇSKI, T. (2024). Microstructure and Mechanical Properties AlSi7Mg Alloy with Sr, Al and AlSi7Mg. *Manufacturing Technology Journal*, Vol. 24, No. 2, pp. 227-234. ISSN 1213-2489
- [12] WANG, F., QIU, D., LIU, Z., TAYLOR, J., EASTON, M., ZHANG, M. (2013). The Grain Refinement Mechanism of Cast Aluminium by Zirconium. *Acta Materialia*, Vol. 61, No. 15, pp. 5636-5645. ISSN 1359-6454
- [13] MATEJKA, M., BOLIBRUCHOVÁ, D., KAJÁNEK, D. (2023). Evaluation of the Corrosion Resistance of the Al-Si-Cu-Mg Alloy with the Addition of Zirconium. *Manufacturing Technology Journal*, Vol. 23, No. 6, pp. 861-869. ISSN 1213-2489

- [14] BOLIBRUCHOVÁ, D., KURIŠ, M., MATEJKA, M., KASÍŇSKA, J. (2022). Study of the Influence of Zirconium, Titanium and Strontium on the Properties and Microstructure of AlSi7Mg0.3Cu0.5 Alloy. *Materials*, Vol. 15, DOI: 10.3390/ma15103709
- [15] BEVILAQUA, W., STADTLANDER, A., FROEHLICH, A. (2020). High-temperature Mechanical Properties of Cast Al-Si-Cu-Mg Alloy by Combined Additions of Cerium and Zirconium. *Materials Research Express*, Vol. 7, No. 2, IOP Publishing. DOI: 10.1088/2053-1591/ab7163
- [16] QIAN, H., ZHU, D., HU, CH., JIANG, X. (2018). Effect of Zr Additive on Microstructure, Mechanical Properties, and Fractography of Al-Si Alloy. *Metals*, Vol. 8, No. 2, DOI: 10.3390/met8020124
- [17] SIGLI, C. (2004). Zirconium Solubility in Aluminum Alloys. *Materials Science Forum*, Vol. 28.
- [18] RAKHMONOV, J., TIMELLI, G., BONOLLO, F. (2016). The Effect of Transition Elements on High-Temperature Mechanical Properties of Al-Si Foundry Alloys-A Review. *Advanced Engineering Materials*, Vol. 18, No. 7, pp. 1096-1105. DOI: 10.1002/adem.201500468
- [19] ŠURDOVÁ, Z., KUCHARIKOVÁ, L., TILLOVÁ, E., PASTIEROVIČOVÁ, L., CHALUPOVÁ, M., UHRIČÍK, M., MIKOLAJČÍK, M. (2022). The Influence of Fe Content on Corrosion Resistance of Secondary AlSi7Mg0.3 Cast Alloy with Increased Fe-content. *Manufacturing Technology Journal*, Vol. 22, No. 5, pp. 598-604. ISSN 1213-2489
- [20] MORRI, A., CESCHINI, L., MESSIERE, S., CERRI, E., TOSCHI, S. (2018). Mo Addition to the A354 (Al-Si-Cu-Mg) Casting Alloy: Effects on Microstructure and Mechanical Properties at Room and High Temperature. *Metals*, Vol. 8, No. 6, DOI: 10.3390/met8060393
- [21] SZYMCZAK, T., GUMIENNY, G., KLIMEK, L. (2020). Characteristics of Al-Si Alloys with High Melting Point Elements for High Pressure Die Casting. *Materials*, Vol. 13, No. 21, DOI: 10.3390/ma13214861
- [22] GRIGORIEV, S., MIRONOV, A., KUZNETSOVA, E., PRISTINSKIY, Y., PODRABINNIK, P., PINARGOTE, N., GERSHMAN, I., PERETYAGIN, P., SMIRNOV, A. (2021). Enhancement of the Mechanical and Tribological Properties of Aluminum-Based Alloys Fabricated by SPS and Alloyed with Mo and Cr. *Metals*, Vol. 11, No. 12, DOI: 10.3390/met11121900
- [23] BRŮNA, M., KUCHARČÍK, L. (2013). Prediction of the Porosity of Al Alloys. *Manufacturing Technology Journal*, Vol. 13, No. 3, pp. 296-302. ISSN 1213-2489
- [24] BOLIBRUCHOVÁ, D., KURIŠ, M., MATEJKA, M. (2019). Effect of Zr on Selected Properties and Porosity of AlSi9Cu1Mg Alloy for the Purpose of Production of High-precision Castings. *Manufacturing technology Journal*, Vol. 19, No. 4, pp. 552-558. ISSN 1213-2489
- [25] VANDERSLUIS, E., EMADI, P., ANDILAB, B., RAVINDRAN, C. (2020) The Role of Silicon Morphology in the Electrical Conductivity and Mechanical Properties of As-Cast B319 Aluminum Alloy. *Metallurgical and Materials Transactions A*, pp. 1874-1886. DOI: 10.1007/s11661-020-05650-2